Supplementary information: DFT-Assisted Polymorph Identification from Lattice Raman Fingerprinting

Natalia Bedoya-Martínez,[*,†] Benedikt Schrode,[†] Andrew O. F. Jones,[†] Tommaso Salzillo,[‡] Christian Ruzié,[¶] Nicola Demitri,[§] Yves H. Geerts,[¶] Elisabetta Venuti,[‡] Raffaele Guido Della Valle,[‡] Egbert Zojer,[†] and Roland Resel[*,†]

†*Institute of Solid State Physics, NAWI Graz, Graz University of Technology, Petersgasse 16, 8010 Graz, Austria*

‡*Department of Industrial Chemistry "Toso Montanari", University of Bologna, Viale Risorgimento 4, I-40136 Bologna, Italy*

¶*Laboratoire de Chimie des Polyméres, Faculté des Sciences, Université Libre de Bruxelles (ULB) CP206/01, Campus de la Plaine, 1050 Brussels, Belgium*

§*Elettra - Sincrotrone Trieste, S.S. 14 Km 163.5 in Area Science Park, 34149 Basovizza - Trieste, Italy*

E-mail: bedoyamartinez@tugraz.at; roland.resel@tugraz.at

C_8O-BTBT-OC_8

C_8O-BTBT-OC_8 was synthesized following the procedure described in literature.[1] The as-synthesized powder was recrystallized from hexane solution, with the re-crystallized powder used to produce the samples presented here. Crystals were grown at room temperature by dissolving C_8O-BTBT-OC_8 powder in hexane slightly below saturation concentration and then allowing the solvent to evaporate. To control the evaporation rate, the vial was either left uncovered or covered by Parafilm with a small hole in it. Lattice phonon Raman spectra were recorded with a Horiba Jobin-Yvon T64000 Triple Monochromator Raman Spectrometer equipped with an Olympus BX40 optical microscope. As incidence light, a 647.1 nm Krypton laser (Coherent Innova 90C) was used. Either a liquid nitrogen or Peltier cooled charge-coupled device (CCD) was used as a detector. The spectrometer was operated with Horiba's LabSpec software. The spectra were calibrated by detection of the 6507 Å line[2–4] of a neon lamp. X-ray diffraction analysis was performed at the X-ray diffraction beamline (XRD1) of the Elettra Synchrotron, Trieste (Italy).[5] Crystals were dipped in NHV oil (Jena Bioscience GmbH) and mounted on the goniometer head with a nylon loop. Complete datasets were collected at room temperature through the rotating crystal method. Data were acquired using monochromatic radiation with a wavelength of 0.700 Å on a Pilatus 2M hybrid-pixel area detector. The diffraction data were indexed and integrated using XDS.[6] Semi-empirical absorption corrections and scaling were performed on datasets, exploiting multiple measures of symmetry-related reflections, using SADABS program.[7] The structure was solved by the dual space algorithm implemented in the SHELXT code.[8] Fourier analysis and refinement were performed by the full-matrix least-squares methods based on F^2 implemented in SHELXL-2016/6.[9] Hydrogen atoms were included at calculated positions with isotropic $U_{factors} = 1.2 \cdot U_{eq}$ or $U_{factors} = 1.5 \cdot U_{eq}$ for methyl groups (U_{eq} being the equivalent isotropic thermal factor of the bonded non-hydrogen atom). Crystals diffracted to a maximum resolution of 1.25 Å, therefore the number of reflections for model fitting was limited and, to avoid over-refinement, anisotropic thermal motion modeling has been applied

only to sulfur and oxygen atoms (the heaviest atoms in the structure). The Coot program was used for structure building.[10]

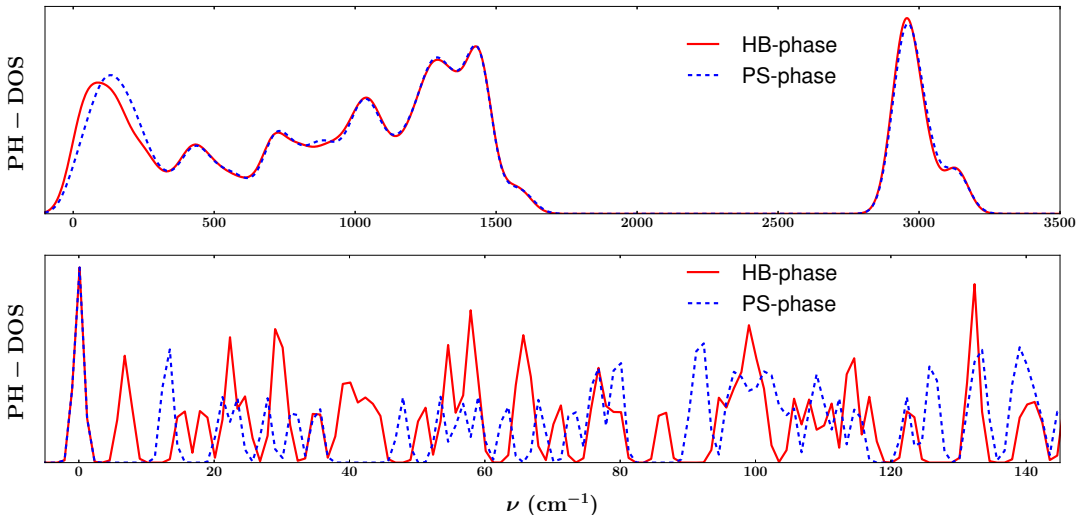

Figure 1s: Phonon density of states of the two polymorphic forms of crystalline C_8O-BTBT-OC_8. Top: comparison of the overall spectra. Bottom: zoom over the lattice phonon regime. Gaussian broadenings of 60 cm^{-1} and 1 cm^{-1}, respectively, are used in these plots.

Simulations were performed in the framework of DFT using the VASP package (version 5.4.1).[11–14] The Perdew-Burke-Ernzerhof (PBE) functional for the exchange and correlation[15] and projector-augmented wave potentials for all the elements were used.[16,17] MBD-vdW corrections were included following the approach of Tkatchenko et al.[18] Calculations were performed using the primitive cell of C_8O-BTBT-OC_8, which contains 148 atoms, and a 6 × 4 × 1 (PS phase) and 1 × 4 × 5 (HB phase) Monkhorst-Pack k-grid to sample the Brillouin zone. The total energy during the self-consistency loop of each DFT step was converged to 10^{-8} eV. Calculations were performed using the experimental unit cell volume, relaxing the atomic positions down to a threshold of 10^{-3} eV $Å^{-1}$ on forces using the GADGET tool.[19] Phonon dispersions were obtained from the force constants using the PHONOPY simulation package.[20] Due to the large simulation cell, all phonon calculations were restricted to the Γ point. The resulting phonon dispersions were subsequently used to calculate Raman intensities, employing the Python program VASP_RAMAN.PY which uses the VASP code as

backend.[21] This program implements the method of Porezag and Pederson[22] to estimate the Raman activity of a vibrational mode. The dependency on temperature of the Raman intensity has been included by using the Bose occupation factor, $1+n(\omega) = [1-\exp(-h\nu_i/k_{\mathrm{B}}T)]^{-1}$, calculated at $T = 300$ K (temperature at which experiments have been performed). The Lorentzian functions around the calculated peak positions on the Raman spectra, Figs. 2c and 2e, were obtained from $I(\nu) = \sum_i I_i \frac{\Gamma}{(\nu-\nu_i)^2+\Gamma^2}$, with $\Gamma = 1.5\,\mathrm{cm}^{-1}$. Here I_i and ν_i are, respectively, the Raman intensity and frequency of a Raman active mode i. k_{B} denotes the Boltzmann constant.

Table 1s: Crystallographic data and refinement details for HB polymorph of the molecule C_8O-BTBT-OC_8.

	C_8O-BTBT-OC_8 HB polymorph
CCDC Number	1557531
Chemical Formula	$C_{60}H_{80}O_4S_4$
Formula weight	993.48 g/mol
Temperature	298(2) K
Wavelength	0.700 Å
Crystal system	Monoclinic
Space Group	P 2_1/c
Unit cell dimensions	$a = 31.056(6)$ Å
	$b = 7.663(2)$ Å
	$c = 5.996(1)$ Å
	$\alpha = 90°$
	$\beta = 94.18(3)°$
	$\gamma = 90°$
Volume	1423.1(5) Å^3
Z	1
Density (calculated)	1.159 g·cm^{-3}

Absorption coefficient	0.200 mm^{-1}
F(000)	536
Crystal size	0.08 × 0.02 × 0.01 mm^3
Crystal habit	Colorless thin plates
Theta range	
for data collection	1.30 to 16.66
Index ranges	-25 ≤ h ≤ 25,
	-6 ≤ k ≤ 6,
	-4 ≤ l ≤ 4
Reflections collected	2641
Independent reflections	806, 473 data with $I > 2\sigma(I)$)
Data multiplicity	
(max resltn)	3.07 (3.30)
$I/\sigma(I)$ (max resltn)	3.40 (1.98)
R_{merge} (max resltn)	0.138 (0.408)
Data completeness	
(max resltn)	98% (100%)
Refinement method	Full-matrix least-squares
	on F^2
Data / restraints / parameters	806/0/79
Goodness-of-fit on F^2	1.014
Δ/σ_{max}	0.000
Final R indices $[I > 2\,\sigma(I)]$	R_1 = 0.0951, wR_2 = 0.2388
R indices (all data)	R_1 = 0.1465, wR_2 = 0.2835
Largest diff. peak and hole	0.331 and -0.250 e·$Å^{-3}$
R.M.S. deviation	
from mean	0.064 e·$Å^{-3}$

$$R_1 = \sum | \, |F_O| \, - |F_C| \, | \, / \, |F_O|, \; wR_2 = \left(\sum [w(F_O^2 - F_C^2)^2] / \sum [w(F_O^2)^2] \right)^{1/2}$$

DB-TTF

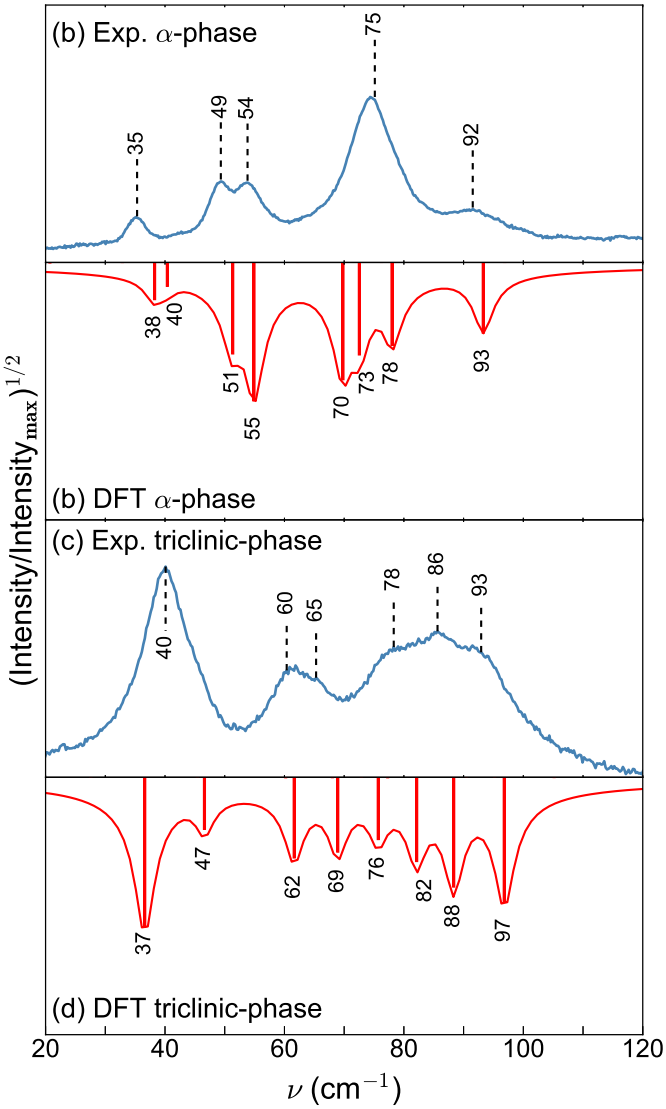

Figure 2s: Experimental Raman spectra of two phases of the molecule DB-TTF: (a) α phase, and (c) triclinic phase, compared against DFT-MBD-vdW calculations (Figs. 2b and 2c, respectively). Experimental data have been taken from Brillante et al. [23,24]

The proposed computational approach has been tested as well for the molecule dibenzo-

tetrathiafulvalene (DB-TTF).[24] Figure 2s shows the calculated Raman spectra, in the energy region below 120 cm^{-1}, of two polymorphs of this molecule compared to experimental data. As it can be seen, the calculated spectra reproduce the experimental measurements with the same accuracy as reported for the C_8O-BTBT-OC_8 molecule (i.e. $\ll 5cm^{-1}$). In this particular case, the resolution of the experimental measurements is limited by the broadening of the Raman peaks, which overlap in regions where active modes are very close to one another. The broadening of the experimental peaks, thus, obscures the richness of the spectra, which can be accessed and visualized using the high accuracy DFT-MBD-vdW simulations.

Simulations were performed following the same approach and convergence criteria as for the C_8O-BTBT-OC_8 molecule. Primitive cells,[23,25] which contain 52 atoms, and a $1 \times 1 \times 3$ (α phase) and $2 \times 2 \times 2$ (triclinic phase) Monkhorst-Pack k-grid to sample the Brillouin zone have been used for the simulations.

References

(1) Ruzié, C.; Karpinska, J.; Laurent, A.; Sanguinet, L.; Hunter, S.; Anthopoulos, T. D.; Lemaur, V.; Cornil, J.; Kennedy, A. R.; Fenwick, O. et al. Design, Aynthesis, Chemical Stability, Packing, Cyclic Voltammetry, Ionisation Potential, and Charge Transport of [1]Benzothieno[3,2-b][1]benzothiophene Derivatives. *J. Mater. Chem. C* **2016**, *4*, 4863–4879.

(2) Fuhr, J. R.; Wiese, W. L. In *NIST Atomic Transition Probability Tables, CRC Handbook of Chemistry & Physics, 77th Edition*; Lide, D. R., Ed.; CRC Press, Inc., Boca Raton, FL, 1996.

(3) Persson, W. The Spectrum of Singly Ionized Neon, Ne II. *Phys. Scr.* **1971**, *3*, 133.

(4) Saloman, E. B.; Sansonetti, C. J. Wavelengths, Energy Level Classifications, and Energy

Levels for the Spectrum of Neutral Neon. *J. Phys. Chem. Ref. Data* **2004**, *33*, 1113–1158.

(5) Lausi, A.; Polentarutti, M.; Onesti, S.; Plaisier, J. R.; Busetto, E.; Bais, G.; Barba, L.; Cassetta, A.; Campi, G.; Lamba, D. et al. Status of the Crystallography Beamlines at Elettra. *Eur. Phys. J. Plus* **2015**, *130*, 43.

(6) Kabsch, W. *XDS*. *Acta Crystallographica Section D* **2010**, *66*, 125–132.

(7) Sheldrick, G. University of Göttingen, Germany.

(8) Sheldrick, G. M. *SHELXT* – Integrated Space-Group and Crystal-Structure Determination. *Acta Cryst. A* **2015**, *71*, 3–8.

(9) Sheldrick, G. M. Crystal Structure Refinement with *SHELXL*. *Acta Cryst. C* **2015**, *71*, 3–8.

(10) Emsley, P.; Lohkamp, B.; Scott, W. G.; Cowtan, K. Features and development of *Coot*. *Acta Cryst. D* **2010**, *66*, 486–501.

(11) Kresse, G.; Hafner, J. Ab initio Molecular Dynamics for Liquid Metals. *Phys. Rev. B* **1993**, *47*, 558–561.

(12) Kresse, G.; Hafner, J. Ab initio Molecular-Dynamics Simulation of the Liquid-MetalAmorphous-Semiconductor Transition in Germanium. *Phys. Rev. B* **1994**, *49*, 14251–14269.

(13) G. Kresse and J. Furthmüller, Efficiency of Ab-Initio Total Energy Calculations for Metals and Semiconductors using a Plane-Wave Basis Set. *Comput. Mater. Sci.* **1996**, *6*, 15 – 50.

(14) Kresse, G.; Furthmüller, J. Efficient Iterative Schemes for Ab Initio Total-Energy Calculations using a Plane-Wave Basis Set. *Phys. Rev. B* **1996**, *54*, 11169–11186.

(15) Perdew, J. P.; Burke, K.; Ernzerhof, M. Generalized Gradient Approximation Made Simple. *Phys. Rev. Lett.* **1996**, *77*, 3865–3868.

(16) Blöchl, P. E. Projector Augmented-Wave Method. *Phys. Rev. B* **1994**, *50*, 17953–17979.

(17) Kresse, G.; Joubert, D. From Ultrasoft Pseudopotentials to the Projector Augmented-Wave Method. *Phys. Rev. B* **1999**, *59*, 1758–1775.

(18) Tkatchenko, A.; DiStasio, R. A.; Car, R.; Scheffler, M. Accurate and Efficient Method for Many-Body van der Waals Interactions. *Phys. Rev. Lett.* **2012**, *108*, 236402.

(19) Bučko, T.; Hafner, J.; Ángyán, J. Geometry Optimization of Periodic Systems Using Internal Coordinates. *J. Chem. Phys* **2005**, *122*.

(20) Togo, A.; Tanaka, I. First Principles Phonon Calculations in Materials Science. *Scr. Mater.* **2015**, *108*, 1–5.

(21) Fonari, A.; Stauffer, S. *vasp_raman.py*; https://github.com/raman-sc/VASP/, 2013.

(22) Porezag, D.; Pederson, M. Infrared Intensities and Raman-Scattering Activities within Density-Functional Theory. *Phys. Rev. B* **1996**, *54*, 7830–7836.

(23) Brillante, A.; Bilotti, I.; Della Valle, R. G.; Venuti, E.; Girlando, A. Probing Polymorphs of Organic Semiconductors by Lattice Phonon Raman Microscopy. *CrystEngComm* **2008**, *10*, 937–946.

(24) Brillante, A.; Bilotti, I.; Valle, R. G. D.; Venuti, E.; Mas-Torrent, M.; Rovira, C.; Yamashita, Y. Phase Recognition by Lattice Phonon Raman Spectra: The Triclinic Structure of the Organic Semiconductor Dibenzo-Tetrathiafulvalene. *Chem. Phys. Lett.* **2012**, *523*, 74 – 77.

(25) Mamada, M.; Yamashita, Y. Triclinic Polymorph of Dibenzotetrathiafulvalene. *Acta Cryst. E* **2009**, *65*, o2083.